

ChemComm

Accepted Manuscript



This is an *Accepted Manuscript*, which has been through the Royal Society of Chemistry peer review process and has been accepted for publication.

Accepted Manuscripts are published online shortly after acceptance, before technical editing, formatting and proof reading. Using this free service, authors can make their results available to the community, in citable form, before we publish the edited article. We will replace this *Accepted Manuscript* with the edited and formatted *Advance Article* as soon as it is available.

You can find more information about *Accepted Manuscripts* in the [Information for Authors](#).

Please note that technical editing may introduce minor changes to the text and/or graphics, which may alter content. The journal's standard [Terms & Conditions](#) and the [Ethical guidelines](#) still apply. In no event shall the Royal Society of Chemistry be held responsible for any errors or omissions in this *Accepted Manuscript* or any consequences arising from the use of any information it contains.

COMMUNICATION

Tuned Red NIR phosphorescence of polyurethane hybrid composites embedding metallic nanoclusters for oxygen sensing.

Cite this: DOI: 10.1039/x0xx00000x

Received 00th January 2012,
Accepted 00th January 2012Maria Amela-Cortes,^{a,b*} Serge Paofai,^a Stéphane Cordier,^a Hervé Folliot^c and Yann Molard^{a,*}

DOI: 10.1039/x0xx00000x

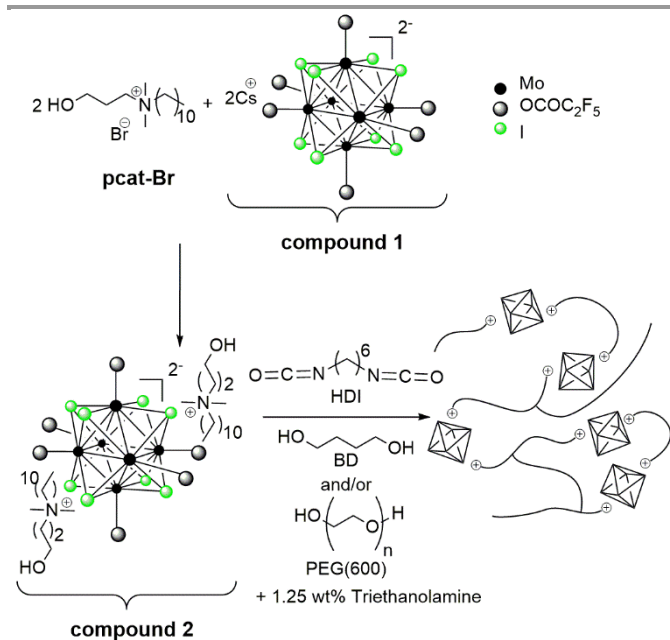
www.rsc.org/

Polyurethane nanocomposites with high content of red NIR luminescent transition metal clusters are presented. The gas permeability of the hybrid material is controlled by playing with the hard/soft segment ratio of the organic matrix structure leading to a drastic and reversible enhancement of the cluster luminescence depending on the molecular oxygen concentration in its surrounding atmosphere.

Phosphorescent materials are of major importance in the development of efficient tools for oxygen sensing or photosensitizer for photodynamic therapy (PDT).^{1, 2} Indeed, as the oxygen ground state is a triplet state, it quenches triplet phosphorescence and generates, in the meantime, singlet oxygen that can be further used in PDT to create new entities toxic for cancer cells. In this frame, nanometric octahedral transition metal cluster units of general formula $[\text{Mo}_6\text{Q}^i_8\text{X}^a_6]^{2-}$ (Q = halogen; X = halogen, organic ligand, i = inner, a = apical), molecular inorganic units obtained as alkali salts by high temperature solid state synthesis, should play a significant role in the near future.³ Indeed, they are highly phosphorescent in the red-NIR area -the most suitable emission bandwidth for biological sensing - under UV or visible excitation, with lifetimes in the range of several tenths of microseconds, possess large Stokes shifts and photoluminescence quantum yields up to 1.⁴ Their long emission lifetimes, is of particular interest to eliminate the organic autofluorescence interferences *via* fluorescence lifetime imaging microscopy,⁵ or time-resolved photoluminescence technique⁶ which opens new prospects for sensing and imaging in various media. The quenching of their phosphorescence was first reported by Jackson *et al.* for $[\text{Mo}_6\text{Q}^i_8\text{X}^a_6]^{2-}$ (Q = Cl, Br; X = Cl, Br, I) who evidenced the formation of singlet oxygen by energy transfer between the

electronically excited $[\text{Mo}_6\text{Q}^i_8\text{X}^a_6]^{2-}$ and molecular oxygen.⁷ They further took advantage of this property by introducing $\text{Mo}_6\text{Cl}_{12}$ into a cross-linked poly(4-vinylpyridine) (PVP) and showed that these systems are efficient oxygen sensors despite the emission lowering due to pyridine coordination onto the six cluster terminal positions.⁸ Gosh *et al.* dispersed the same precursor in a Poly(1-trimethylsilyl-1-propyne) matrix to developed a Mo_6 cluster based silica optical fiber.⁹ From these examples, it is clear that the embedment of these phosphorescent dyes in polymer matrices is a very good mean to take advantage of their luminescence properties. However, the simple dispersion of inorganic moieties in an organic host matrix usually leads to phase segregation because the inorganic and organic parts are not closely bound.¹⁰ Thus, several challenges arise to design hybrid organic inorganic materials that take advantage of cluster phosphorescence while maximizing biocompatibility, detection efficiency and stability. On one hand, ionic assembling¹¹ seems one of the most promising technique compared to the covalent approach^{7, 12} to i) homogeneously introduce high cluster content in polymers, ii) keep the cluster units integrity and thus preserve their emissive properties in the final hybrid material. This approach consists in replacing the alkali counter cations of the anionic cluster unit by functional organic ones able to copolymerize with the chosen organic monomers. On the other hand, polyurethanes (PU) are a versatile class of polymers whose mechanical properties and oxygen permeability can be tailored by varying their chemical composition to meet a wide variety of applications such as coatings, foams, elastomers and biomaterials.^{13, 14} We present herein the first PU hybrid nanocomposites obtained by bulk copolymerization and containing up to 50 wt% of tailored made polymerizable metallic cluster complexes. By introducing a highly luminescent cluster unit such as

$[\text{Mo}_6\text{I}_8(\text{OCOC}_2\text{F}_5)_6]^{2-}$, we expect a high sensitivity of the nanocomposite toward its environment. We also demonstrate that, as the hybrid oxygen permeability can be tailored by playing with the copolymer structure,¹⁵ the emission sensitivity can also be adjusted. In particular, the structural characteristics of the diol components, rigidity for the 1,4-butanediol (BD), and/or flexibility for the Polyethyleneglycol (PEG, $M_w = 600 \text{ g mol}^{-1}$) (Scheme 1), has a great influence on the polymer morphology (crystalline polymers or segmented block copolymers) which impacts on the oxygen permeability and thus on the PU nanocomposite ability to emit light.



Scheme 1 Synthesis of polymerizable cluster 2 and scheme of polymerization.

Here, compound 2 was obtained by a metathesis reaction in an acetone solution between the brominated polymerizable organic salt pcat-Br and compound 1, the cesium salt of the chosen cluster unit. The organic counter-cation (pcat⁺) bears one short alkyl chain terminated by a hydroxyl group and thus, capable of reacting, by step-wise polymerization with diisocyanate groups to form PU copolymers. The bromine salt of this cation was synthesized in one step reaction starting from dimethylaminoethanol and 11-bromoundecane followed by precipitation by addition of diethylether. All molecular compounds were identified by ¹H-NMR, ¹⁹F-NMR, EDAX and elemental analysis.

The synthesis of nanocomposites was performed in one-step bulk polymerization¹⁶ using hexamethylenediisocyanate (HDI), compound 2 and BD or, a mixture of BD and PEG as chain extender. In all polymerizations, 1.25 wt% of triethanolamine (TEA) was used as cross-linker. The formulations of hybrids are shown in Table 1 and were calculated so that a stoichiometric amount of NCO and OH reacting groups were present. For polymers containing only BD as chain extender (PUxH samples with x = compound 2 content = 0, 1, 10, 20, 50), hard orange solids were obtained. In order to produce elastic nanocomposites and increase the oxygen permeability, PEG was introduced in the formulation (PUxF samples with x = compound

2 content = 0, 1, 10, 20, 50). In this way, segmented PU hybrids, containing hard and soft domains in their structure were produced. The soft domains given by PEG provide elastomeric character to the polymer while the hard segments afforded by BD restrain the motion of the soft segment and act as physical cross-linkers.¹³ In a first attempt to produce elastic films, 2 was added in the hard segment replacing appropriate amounts of BD. In this way, a viscous polymer was obtained when 20 and 50 wt% of 2 was used, although the presence of cross-linker. Decreasing the amount of BD induced the disruption of hard domains and thus, the decrease of the dimensional stability. Indeed, when 2 was added in substitution of PEG (soft domain), rubbery films were obtained. For this reason the percentage of BD was fixed to 6 wt% of the total polymer. The flexible samples were obtained after curing the polymers for 24 h at 80 °C in an oven. The influence of the cluster concentration on the thermal behaviour of PU hybrids, hard (PUxH) or flexible (PUxF), was studied by DSC and TGA analysis (ESI fig. S1-S4 and Table S1).

Table 1 Composition and thermal properties of nanocomposite samples.

Sample	2 (wt.%)	BD (wt.%)	PEG (wt.%)	HDI (wt.%)	T _d (°C)	inorganic wt%
PU0H	0	35	0	65	457	0
PU1H	1	35	0	65	466	2
PU10H	10	30	0	60	394	9
PU20H	20	27	0	53	432	14
PU50H	50	18	0	32	434	33
PU0F	0	6	63	30	472	0
PU1F	1	6	62	30	457	2
PU10F	10	6	52	27	459	9
PU20F	20	6	46	27	448	17
PU50F	50	6	18	26	442	43

The DSC thermograms of the segmented elastic polyurethane films showed only a T_g between -40 and -50°C in the first cooling and second heating cycles while PUxH samples showed two endothermic transitions on the first heating and only one on subsequent cooling and heating cycles corresponding to the hybrid melting. This behavior was already described for other non-segmented polyurethane systems and it has to be noted that the appearance, shape and size of these endothermic transitions strongly depend on the synthesis and annealing time and temperatures of the polymers.¹⁷ The decomposition temperatures and the final inorganic content are summarised in Table 1. All decomposition temperatures are in the range of 400–470 °C. In fact, the degradation of PU is a multi-stage process whose complexity increases with the Mo₆ cluster content. For samples containing 10, 20 and 50 wt% of polymerizable cluster building blocks, a weight loss corresponding to the degradation of the six pentafluorobutyrate ligands appears around 250°C. This loss was obviously not detected for 1 wt% containing samples. For PUxF polymers, two other steps were detected at 300 °C and around 380–400 °C. An additional step was observed for PUxH samples around 325 °C that is attributed to the degradation of hard domains. A second step of weight loss for PU10H, PU20H and PU50H was observed at starting temperatures of 287, 270 and 260 °C, respectively which indicates that the addition of Mo₆ cluster unit destabilises the hard segment microdomains.

Photoluminescence properties were investigated in the solid state with all nanocomposite samples and compared to the one of their

parent cluster precursor. **Figure 1a** shows PUxF ($x = 1, 10, 20$) samples under UV irradiation at 365 nm (see ESI Fig S5 for emission spectra). All samples show the same broad and structureless emission band between 550 and 950 nm typical of the cluster core upon excitation anywhere in their absorption band ($\lambda = 300\text{-}550$ nm). The introduction of clusters into the PU matrix has only little influence, qualitatively, on their emission properties. Indeed, a slight red shift from around 10 nm to 20 nm in the emission maximum could be observed. This point is in good accordance with the preservation of the cluster anionic unit physical integrity within the copolymer. Quantitative luminescence studies were realized in air and N₂ atmosphere to study the oxygen sensitivity of hybrid nanocomposites in the solid state. The absolute quantum yield values were calculated by irradiating samples in an integrating sphere which internal atmosphere was controlled toward a gas inlet. The results are summarized in **Table 2**.

Table 2 Phosphorescence absolute quantum yield values of compound 2, PU powders (PUxH) and films (PUxF) samples under air or nitrogen atmosphere

Samples	λ_{max} (nm)	ϕ_{em} (air)	ϕ_{em} (N ₂)
2	654	0.05	0.80
PU1H	678	0.18	0.20
PU10H	669	0.15	0.18
PU20H	666	0.30	0.32
PU50H	670	0.07	0.11
PU1F	674	0.08	0.38
PU10F	674	0.08	0.36
PU20F	674	0.11	0.40
PU50F	660	0.10	0.70

As mentioned earlier, Mo₆ clusters bearing fluorinated groups in apical position are highly emissive showing an emission absolute quantum yield in the solid state of 0.35 in air. Compound **2** presents a ϕ_{em} of only 0.05 in the same experimental conditions. Once air was replaced by nitrogen, this value raised up to 0.80. However, we observed that the ϕ_{em} of the PUxH hybrids was poorly affected by their surrounding atmospheric environment. This can be explained by the low permeability to gases of the crystalline hard domain polymers. In contrast, the flexible hybrids, containing both hard and soft segments because of the addition of PEG (PuxF samples), are indeed permeable to gases and different ϕ_{em} values were calculated under air or nitrogen atmosphere. Hence, all PUxF samples presented a fairly low ϕ_{em} of around 0.10 under air and reached around 0.40 under nitrogen atmosphere for polymers containing up to 20 wt% of cluster. For PU50F, the ϕ_{em} under nitrogen reached 0.70. The reason why polymers containing lower cluster content do not reach the same value as PU50F may be explained by the ability of the organic matrix to absorb part of the excitation light. However, the huge difference of AQY value between PU50H and other powdered samples remains still unexplained. To assess about the stability and reversibility of the oxygen quenching phenomenon, fatigue studies were investigated by measuring the absolute quantum yields during several cycles under normal and inert atmosphere. Although we were not able to control precisely the amount of oxygen within our experimental set up (off/on state were in the contrary very well mastered), we noticed a very quick enhancement of the hybrid emissive ability under N₂ gas flow (see the video in ESI that illustrates the high sensitivity of PU50F photoluminescence toward the application of a N₂ stream). In our

conditions, half of the emission enhancement appeared in less than 5 seconds under gas flow while 90 % of it was reached after 55 seconds (see ESI Figure S6). Nonetheless, values were recorded after 300 s under gas flow to assess about the emission stability. **Figure 1b** presents the results for PU50F while inset shows the PU50F sample under irradiation in air and N₂ atmosphere (results for other hybrids are presented in ESI Fig S7). It turns out that, the permeability of the polymer matrix induces a full reproducibility of the luminescence quenching/enhancement phenomenon. Phosphorescence decay profiles were obtained in air and when a N₂ stream was directed toward the samples for PU1F, PU10F and PU50F (see ESI Figure S8-S10). In all cases, the data were fitted to a two-exponential decay with a short lifetime around 10 μs and a longer one of several tenths of microseconds. The longer lifetime value increases slightly upon application of a N₂ stream,. This expected variation illustrates the usual behaviour of the dynamic quenching by molecular oxygen of phosphorescent dyes.¹

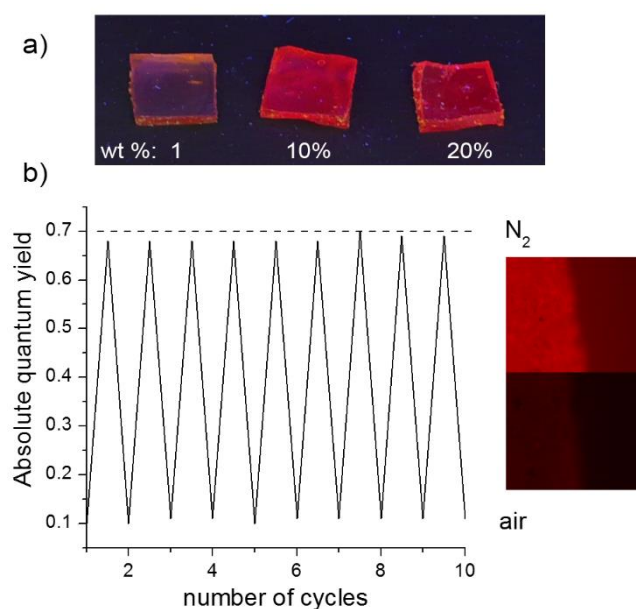


Fig. 1 a) PU hybrid films under UV light, b) Evolution of the absolute quantum yield value of PU50F films under air/N₂ atmosphere cycling. right: pictures of PU50F sample under UV irradiation in air (bottom) and in N₂ (top) enriched atmosphere (integration time: 100ms).

In conclusion, we first demonstrate in this work the versatility of the ionic technique to introduce highly luminescent metallic clusters in any type of polymer matrix. [Mo₆I₈(OCOC₂F₅)₆]²⁻ cluster unit was functionalized with a tailor made organic counter cation designed to integrate the inorganic phosphor in a polyurethane nanocomposite. By this method, up to 50 wt% of polymerizable cluster units could be introduced in the copolymer. Then, by playing with the nanocomposite formulation and more particularly with the hard/soft segments ratio, hard and flexible samples were prepared. Quantitative emission studies reveal that film samples show a high gas permeability which allow to drastically modify the ability of metallic clusters to emit. By passing from an air to a N₂ atmosphere, a spectacular and reversible enhancement of the absolute quantum yield value from 0.10 to 0.7 is observed with the most doped PU. These

nanocomposites, because of the biocompatibility of the organic matrix and the tremendous ability of the inorganic counter-part to be quenched by molecular oxygen, offer great promises in the design of efficient oxygen sensors or as sensitizer in photodynamic therapy.

This work was realized in the frame of the PHYSTER maturation program financed by Region Bretagne and FEDER, and, partially in the frame of the ANR-13-BS07-0003-01.

Notes and references

“Université de Rennes 1- CNRS UMR 6226“Institut des Sciences Chimiques de Rennes“, Campus de Beaulieu, CS 74205, 35042 Rennes Cedex, France. yann.molard@univ-rennes1.fr, maria.amela-cortes@univ-rennes1.fr

b) SATT Ouest-Valorisation, 14C Rue du Pâtis Tatelin, Metropolis 2, CS 80 804, 35708, Rennes Cedex (France)

c) Université Européenne de Bretagne, INSA, FOTON, UMR 6082, F-35708 Rennes, France.

Electronic Supplementary Information (ESI) available: synthetic procedures and analytical data, DSC and TGA thermograms and related detailed discussion, luminescence spectra of all samples, phosphorescence decay profiles and fits. See DOI: 10.1039/c000000x/

- X.-d. Wang and O. S. Wolfbeis, *Chem. Soc. Rev.*, 2014, **43**, 3666.
- X.-L. Qi, S.-Y. Liu, R.-B. Lin, P.-Q. Liao, J.-W. Ye, Z. Lai, Y. Guan, X.-N. Cheng, J.-P. Zhang and X.-M. Chen, *Chem. Commun.*, 2013, **49**, 6864; C. O'Donovan, J. Hynes, D. Yashunski and D. B. Papkovsky, *J. Mater. Chem.*, 2005, **15**, 2946; A. P. Castano, P. Mroz and M. R. Hamblin, *Nat. Rev. Cancer*, 2006, **6**, 535.
- S. Cordier, F. Grasset, Y. Molard, M. Amela-Cortes, R. Boukherroub, S. Ravaine, M. Mortier, N. Ohashi, N. Saito and H. Haneda, *J. Inorg. Organomet. Polym. Mater.*, 2015, **25**, 189; A. A. Krasilnikova, M. A. Shestopalov, K. A. Brylev, I. A. Kirilova, O. P. Khripko, K. E. Zubareva, Y. I. Khripko, V. T. Podorognaya, L. V. Shestopalova, V. E. Fedorov and Y. V. Mironov, *J. Inorg. Biochem.*, 2015, **144**, 13; S. Cordier, Y. Molard, K. A. Brylev, Y. V. Mironov, F. Grasset, B. Fabre and N. G. Naumov, *J. Cluster Sci.*, 2015, **26**, 53; K. Kirakci, S. Cordier and C. Perrin, *Z. Anorg. Allg. Chem.*, 2005, **631**, 411; F. A. Cotton and N. F. Curtis, *Inorg. Chem.*, 1965, **4**, 241.
- A. W. Maverick and H. B. Gray, *J. Am. Chem. Soc.*, 1981, **103**, 1298; A. W. Maverick, J. S. Najdzionek, D. MacKenzie, D. G. Nocera and H. B. Gray, *J. Am. Chem. Soc.*, 1983, **105**, 1878; M. N. Sokolov, M. A. Mihailov, E. V. Peresyphina, K. A. Brylev, N. Kitamura and V. P. Fedin, *Dalton Trans.*, 2011, **40**, 6375; K. Kirakci, P. Kubat, M. Dusek, K. Fejfarova, V. Sicha, J. Mosinger and K. Lang, *Eur. J. Inorg. Chem.*, 2012, 3107.
- G. Zhang, H. Zhang, Y. Gao, R. Tao, L. Xin, J. Yi, F. Li, W. Liu and J. Qiao, *Organometallics*, 2014, **33**, 61; M. Yu, Q. Zhao, L. Shi, F. Li, Z. Zhou, H. Yang, T. Yi and C. Huang, *Chem. Commun.*, 2008, 2115.
- H. Shi, H. Sun, H. Yang, S. Liu, G. Jenkins, W. Feng, F. Li, Q. Zhao, B. Liu and W. Huang, *Adv. Funct. Mater.*, 2013, **23**, 3268; Y. Ma, S. Liu, H. Yang, Y. Wu, H. Sun, J. Wang, Q. Zhao, F. Li and W. Huang, *J. Mater. Chem. B*, 2013, **1**, 319.
- J. A. Jackson, C. Turro, M. D. Newsham and D. G. Nocera, *J. Phys. Chem.*, 1990, **94**, 4500.
- J. A. Jackson, M. D. Newsham, C. Worsham and D. G. Nocera, *Chem. Mater.*, 1996, **8**, 558; R. Ramirez-Tagle and R. Arratia-Perez, *Chem. Phys. Lett.*, 2009, **475**, 232.
- R. N. Ghosh, G. L. Baker, C. Ruud and D. G. Nocera, *Appl. Phys. Lett.*, 1999, **75**, 2885.
- B. Moraru, N. Huesing, G. Kickelbick, U. Schubert, P. Fratzl and H. Peterlik, *Chem. Mater.*, 2002, **14**, 2732; S. Gross, V. Di Noto and U. Schubert, *J. Non-Cryst. Solids*, 2003, **322**, 154.
- M. Amela-Cortes, S. Cordier, N. G. Naumov, C. Mériadec, F. Artzner and Y. Molard, *J. Mater. Chem. C*, 2014, **2**, 9813; M. A. Amela-Cortes, F. Dorson, M. Prévôt, A. Ghoufi, B. Fontaine, F. Goujon, R. Gautier, V. Cîrcu, C. Mériadec, F. Artzner, H. Folliot, S. Cordier and Y. Molard, *Chem. Eur. J.*, 2014, **20**, 8561; A. S. Mocanu, M. Amela-Cortes, Y. Molard, V. Cîrcu and S. Cordier, *Chem. Commun.*, 2011, **47**, 2056; Y. Molard, F. Dorson, V. Cîrcu, T. Roisnel, F. Artzner and S. Cordier, *Angew. Chem. Int. Ed.*, 2010, **49**, 3351; Y. Molard, A. Ledneva, M. Amela-Cortes, V. Cîrcu, N. G. Naumov, C. Mériadec, F. Artzner and S. Cordier, *Chem. Mater.*, 2011, **23**, 5122; M. Amela-Cortes, A. Garreau, S. Cordier, E. Faulques, J.-L. Duvail and Y. Molard, *J. Mater. Chem. C*, 2014, **2**, 1545.
- J. H. Golden, H. Deng, F. J. DiSalvo, J. M. J. Fréchet and P. M. Thompson, *Science*, 1995, **268**, 1463; L. M. Robinson and D. F. Shriver, *J. Coord. Chem.*, 1996, **37**, 119; O. A. Adamenko, G. V. Lukova, N. D. Golubeva, V. A. Smirnov, G. N. Boiko, A. D. Pomogailo and I. E. Uflyand, *Dokl. Phys. Chem.*, 2001, **381**, 275; O. A. Adamenko, G. V. Loukova and V. A. Smirnov, *Russ. Chem. Bull.*, 2002, **51**, 994; Y. Molard, F. Dorson, K. A. Brylev, M. A. Shestopalov, Y. Le Gal, S. Cordier, Y. V. Mironov, N. Kitamura and C. Perrin, *Chem. Eur. J.*, 2010, **16**, 5613; Y. Molard, C. Labbé, J. Cardin and S. Cordier, *Adv. Funct. Mater.*, 2013, **23**, 4821; O. A. Efremova, K. A. Brylev, O. Kozlova, M. S. White, M. A. Shestopalov, N. Kitamura, Y. V. Mironov, S. Bauer and A. J. Sutherland, *J. Mater. Chem. C*, 2014, **2**, 8630.
- S. Desai, I. M. Thakore, B. D. Sarawade and S. Devi, *Eur. Polym. J.*, 2000, **36**, 711.
- M. A. Hood, B. Wang, J. M. Sands, J. J. La Scala, F. L. Beyer and C. Y. Li, *Polymer*, 2010, **51**, 2191; A. Mishra, B. P. D. Purkayastha, J. K. Roy, V. K. Aswal and P. Maiti, *Macromolecules*, 2010, **43**, 9928.
- J. S. McBride, T. A. Massaro and S. L. Cooper, *J. Appl. Polym. Sci.*, 1979, **23**, 201; K. Matsunaga, K. Sato, M. Tajima and Y. Yoshida, *Polym J*, 2005, **37**, 413.
- A. Sirkecioglu, H. B. Mutlu, C. Citak, A. Koc and F. S. Güner, *Polym. Eng. Sci.*, 2014, **54**, 1182.
- C. M. Brunette, S. L. Hsu and W. J. MacKnight, *Macromolecules*, 1982, **15**, 71.